J|A|C|S
ARTICLES
Published on Web 09/19/2002

Solution NMR Techniques for Large Molecular and Supramolecular Structures

Roland Riek,[†,§] Jocelyne Fiaux,[†] Eric B. Bertelsen,[‡] Arthur L. Horwich,[‡] and Kurt Wüthrich*[,†]

Contribution from the Institut für Molekularbiologie und Biophysik, Eidgenössische Technische Hochschule Zürich, CH-8093 Zürich, Switzerland, and Howard Hughes Medical Institute and Department of Genetics, Yale School of Medicine, New Haven, Connecticut 06510

Received May 2, 2002

Abstract: Transverse relaxation-optimized spectroscopy (TROSY) or generation of heteronuclear multiple quantum coherences during the frequency labeling period and TROSY during the acquisition period have been combined either with cross-correlated relaxation-induced polarization transfer (CRIPT) or cross-correlated relaxation-enhanced polarization transfer (CRINEPT) to obtain two-dimensional (2D) solution NMR correlation spectra of ^{15}N,^{2}H-labeled homo-oligomeric macromolecules with molecular weights from 110 to 800 kDa. With the experimental conditions used, the line widths of the TROSY-components of the ^{1}H- and ^{15}N-signals were of the order of 60 Hz at 400 kDa, whereas, for structures of size 800 kDa, the line widths were about 75 Hz for ^{15}N and 110 Hz for ^{1}H. This paper describes the experimental schemes used and details of their setup for individual measurements. The performance of NMR experiments with large structures depends critically on the choice of the polarization transfer times, the relaxation delays between subsequent recordings, and the water-handling routines. Optimal transfer times for 2D [^{15}N,^{1}H]-CRIPT-TROSY experiments in H_2O solutions were found to be 6 ms for a molecular weight of ~200 kDa, 2.8 ms for 400 kDa, and 1.4 ms for 800 kDa. These data validate theoretical predictions of inverse proportionality between optimal transfer time and size of the structure. The proton longitudinal relaxation times in H_2O solution were found to be of the order of 0.8 s for structure sizes around 200 kDa, 0.4 s at 400 kDa, and 0.3 s at 800 kDa, which enabled the use of recycle times below 1 s. Since improper water handling results in severe signal loss, the water resonance was kept along the *z*-axis during the entire duration of the experiments by adjusting each water flip-back pulse individually.

Introduction

NMR structure determination of small proteins and nucleic acid fragments is well established in biological and biochemical research.[2] With further progress in structural biology and the emergence of structural and functional genomics, it is of keen interest to develop novel NMR techniques that enable solution NMR studies also with larger structures. The recently developed principles of TROSY (transverse relaxation-optimized spectroscopy)[3] and CRINEPT (cross-correlated relaxation-enhanced polarization transfer)[4] provide a basis for such projects. This publication gives a guideline for two-dimensional (2D) NMR measurements with very large structures, using ^{15}N,^{2}H-labeled homo-oligomeric proteins with molecular weights of 110 to 800 kDa as examples for an optimal selection of the relaxation delay and the polarization transfer and frequency labeling periods. During polarization transfer and frequency labeling, transverse relaxation has a dominant impact on the sensitivity and resolution of the NMR experiments, whereas the longitudinal relaxation rate is the dominant factor to be considered when deciding on the length of the relaxation delay. Deuterium-labeling and the use of TROSY[3] reduce transverse relaxation during frequency labeling periods, and CRINEPT-type polarization transfers[4] further increase the sensitivity of the NMR experiments. An additional critical aspect is proper water handling,[5] which needs precise optimization in each individual experiment.

Materials

The NMR experiments were recorded with protein solutions for which the preparation has either been described previously or will be

* Address correspondence to this author: wuthrich@mol.biol.ethz.ch.
† Eidgenössische Technische Hochschule.
‡ Yale School of Medicine.
§ Present address: Structural Biology Laboratory, The Salk Institute, 10010 N. Torrey Pines Rd., La Jolla, CA 92037.

(1) Abbreviations: COSY, correlation spectroscopy; CRINEPT, cross-correlated relaxation-enhanced polarization transfer; CRIPT, cross-correlated relaxation-induced polarization transfer; CSA, chemical shift anisotropy; DHNA, 7,8-dihydroneopterin aldolase; INEPT, insensitive nuclei enhanced by polarization transfer; DD, dipole−dipole; HMQC, heteronuclear multiple-quantum correlation; SR1, single-ring variant of GroEL with seven subunits; TROSY, transverse relaxation-optimized spectroscopy; 2D and 3D, two- and three-dimensional.

(2) Wüthrich, K. *NMR of Proteins and Nucleic Acids;* Wiley: New York, 1986.
(3) Pervushin, K.; Riek, R.; Wider, G.; Wüthrich, K. *Proc. Natl. Acad. Sci. U.S.A.* **1997**, *94*, 12366−12371.
(4) Riek, R.; Wider, G.; Pervushin, K.; Wüthrich, K. *Proc. Natl. Acad. Sci. U.S.A.* **1999**, *96*, 4918−4923.
(5) Piotto, M.; Saudek, V.; Sklenar, V.; *J. Biomol. NMR* **1992**, *2*, 661−665. Grzesiek, S.; Bax, A. *J. Am. Chem. Soc.* **1993**, *115*, 12593−12594. Talluri, S.; Wagner, G. *J. Magn. Reson. B* **1996**, *112*, 200−205.

10.1021/ja026763z CCC: $22.00

described elsewhere: (i) Uniformly $^{15}N,^{2}H$-labeled GroEL from *E. coli*. Measurements were performed at pH 6.1 and at a protein concentration of 0.1 mM (1.4 mM per subunit) in a mixed solvent containing 95% H_2O/5% $^{2}H_2O$ with 25 mM potassium phosphate and 20 mM KCl. GroEL is a homotetradecamer, with a total molecular weight of 800 kDa and 547 amino acid residues per subunit.[6] X-ray crystallography has shown that all subunits are symmetry-related.[7] (ii) [98% ^{15}N; *U*-85% ^{2}H]-labeled SR1. Measurements were performed at pH 6.1 and at a protein concentration of 0.2 mM (1.4 mM per subunit) in 95% H_2O/5% $^{2}H_2O$ with 25 mM potassium phosphate and 20 mM KCl. SR1 is a single-ring variant of GroEL, with seven subunits and an overall molecular size of 400 kDa.[8] (iii) Uniformly $^{15}N,^{2}H$-labeled GroES bound to uniformly ^{2}H-labeled SR1. Measurements were performed at pH 6.1 and at a complex concentration of 0.15 mM in isotope-labeled GroES in 95% H_2O/5% $^{2}H_2O$ with 25 mM potassium phosphate and 20 mM KCl. GroES is a homoheptameric protein with a molecular weight of 72 kDa and 97 amino acid residues per subunit.[6,9] X-ray crystallography indicates that the subunits are symmetry-related in their well-defined regions.[10] (iv) [98% ^{15}N; *U*-85% ^{2}H]-labeled 7,8-dihydroneopterin aldolase (DHNA) from *Staphylococcus aureus*. Measurements were performed at pH 6.5 and at a protein concentration of 0.5 mM (4 mM per subunit) in a mixed solvent of 95% H_2O/5% $^{2}H_2O$ with 75 mM deuterated ammonium acetate.[11] DHNA is a homo-octamer of 110 kDa, with 121 amino acid residues per subunit. X-ray crystallography has shown that all subunits are symmetry-related.[12] (v) Uniformly $^{15}N,^{2}H$-labeled N-terminal 43 kDa fragment of the β-subunit of the gyrase from *Staphylococcus aureus*.[13] Measurements were performed at pH 8.6. and at a protein concentration of 1 mM in 95% H_2O/5% $^{2}H_2O$.

Methods

When compared to corresponding experiments commonly used for studies with structures of molecular weights in the range 10−30 kDa,[14] the following are novel traits of the 2D $^{15}N,^{2}H$-correlation NMR experiments designed for studies of large structures: (i) The 90° (^{1}H) pulse length cannot conveniently be determined with conventional approaches.[15] Therefore, it was calibrated with a pulse sequence of a single hard pulse phase shifted by 45° relative to the phase of the acquisition, during which the real and imaginary parts of the free induction decay are recorded simultaneously. The pulse is exactly 180° when the first points of both the real and imaginary parts of the free induction decay are zero (M. Salzmann, private communication). (ii) For optimal sensitivity, the water magnetization was kept along the *z*-axis during the entire duration of the NMR experiments, using water-selective pulses.[5] Improper water handling results in severe signal loss (Figure 1), indicating a strong correlation between the water magnetization and the ^{1}H magnetization of large structures. (iii) The polarization transfers are based on cross-correlated relaxation, which becomes an efficient transfer mechanism for structures in the range above 200 kDa. Since high field strength B_0 benefits TROSY as well as CRINEPT,[3,4,16] the NMR experiments were recorded on a Bruker DRX750 MHz spectrometer using a triple-resonance probe with an actively shielded z-gradient coil. Details of the data handling after acquisition are given in the figure captions for the individual experiments. Specific features of the water handling techniques and of individual one- and two-dimensional NMR experiments for use with very large structures are discussed in the following.

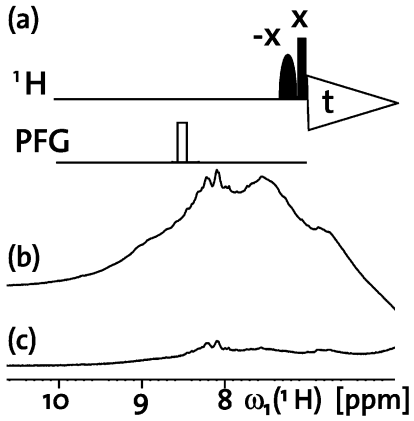

Figure 1. 1D ^{1}H NMR spectroscopy with the uniformly $^{15}N,^{2}H$-labeled 800-kDa protein GroEL. (a) 1D ^{1}H NMR pulse sequence. (b) 1D ^{1}H NMR spectrum measured with the pulse sequence in the scheme of part a. (c) 1D ^{1}H NMR spectrum measured using a 1D experiment with water suppression by saturation during the entire relaxation delay prior to the 90°(^{1}H) pulse (in parts b and c, ^{1}H frequency = 750 MHz, acquisition time = 100 ms, and interscan delay = 0.3 s). Before the 90° hard pulse, part a includes a Gaussian-shaped water-selective 90° pulse with a length of 1.1 ms. In addition, a pulsed magnetic field gradient with a duration of 1 ms and an amplitude of 10 G/cm was applied during the interscan delay.

Water Suppression in NMR Experiments with Large Structures. In NMR experiments with large structures, the water magnetization must be along the *z*-axis during the entire duration of the measurement. Improper water handling results in a dramatic decrease in sensitivity over the whole spectral width, as demonstrated here with one-dimensional (1D) ^{1}H NMR spectra of uniformly $^{15}N,^{2}H$-labeled GroEL (Figure 1). In each NMR experiment, we adjusted each water-selective pulse[5] individually for optimal water flip-back quality. For example, since radiation damping tends to oppose driving the water magnetization from the $+z$-axis to the transverse plane,[17] such as by the first soft pulse in Figure 2a, higher power for the selective water pulse will be required than that when returning the water to the $+z$ axis, such as by the second soft pulse in Figure 2a, where radiation damping supports the soft pulse.[17]

One-Dimensional ^{1}H NMR Experiments. Figure 1a for 1D ^{1}H NMR experiments with large structures contains a water-selective $90°_{-x}$ pulse followed by a $90°_{x}$ hard pulse, so that the water magnetization is along the $+z$-axis during the signal acquisition period *t*. A pulsed magnetic field gradient is applied during the interscan delay to destroy possible residual in-phase magnetization.

Two-Dimensional [$^{15}N,^{1}H$]-CRIPT-TROSY. The 2D [$^{15}N,^{1}H$]-CRIPT-TROSY experiment (Figure 2a) is transverse relaxation-optimized for its entire duration (Table 1). It uses TROSY[3] during the evolution and acquisition periods and CRIPT[4] for the polarization transfer. 2D [$^{15}N,^{1}H$]-CRIPT-TROSY starts with the ^{1}H magnetization generated by the first 90°(^{1}H) pulse, which is then transferred to heteronuclear antiphase magnetization, using cross-correlated relaxation

(6) Hendrix, R. W. *J. Mol. Biol.* **1979**, *129*, 375−392. Hohn, T.; Hohn, B.; Engel, A.; Wurtz, M.; Smith, P. R. *J. Mol. Biol.* **1979**, *129*, 359−373. Hemmingsen, S. M.; Woolford, C.; van der Vies, S. M.; Tilly, K.; Dennis, D. T.; Georgopoulos, C. P.; Hendrix, R. W.; Ellis, R. J. *Nature* **1988**, *333*, 330−334.
(7) Sigler, P. B.; Xu, Z.; Rye, H. S.; Burston, S. G.; Fenton, W.; Horwich, A. L. *Annu. Rev. Biochem.* **1998**, *67*, 581−608.
(8) Horwich, A. L.; Burston, S. G.; Rye, H. S.; Weissman, J. S.; Fenton, W. A. *Methods Enzymol.* **1998**, *290*, 141−146.
(9) Chandrasekhar, G. N.; Tilly, K.; Woolford, C.; Hendrix, R.; Georgopoulos, C. *J. Biol. Chem.* **1986**, *261*, 12414−12419.
(10) Hunt, J. F.; Weaver, A. J.; Landry, S. J.; Gierasch, L.; Deisenhofer, J. *Nature* **1996**, *379*, 37−45.
(11) Salzmann, M.; Pervushin, K.; Wider, G.; Senn, H.; Wüthrich, K. *J. Am. Chem. Soc.* **2000**, *122*, 7543−7548.
(12) Hennig, M.; D′Arcy, A.; Hampele, I. C.; Page, M. G.; Oefner, C.; Dale, G. E. *Nat. Struct. Biol.* **1998**, *5*, 357−62.
(13) Andersson, P.; Annila, A.; Otting, G. *J. Magn. Reson.* **1998**, *133*, 364−367. Wider, G.; Wüthrich, K. *Curr. Opin. Struct. Biol.* **1999**, *9*, 594−601.
(14) Bax, A.; Grzesiek, S. *Acc. Chem. Res.* **1993**, *26*, 131−138. Wider, G. *Prog. Nucl. Magn. Reson. Spectrosc.* **1998**, *32*, 193−275.
(15) Cavanagh, J.; Fairbrother, W. J.; Palmer, A. G., III; Skelton, N. J. *Protein NMR Spectroscopy*; Academic Press: San Diego, CA, 1996.
(16) Wüthrich, K. *Nat. Struct. Biol.* **1998**, *5*, 492−495.
(17) Chen, J. H.; Jerschow, A.; Bodenhausen, G. *Chem. Phys. Lett.* **1999**, *308*, 397−402.

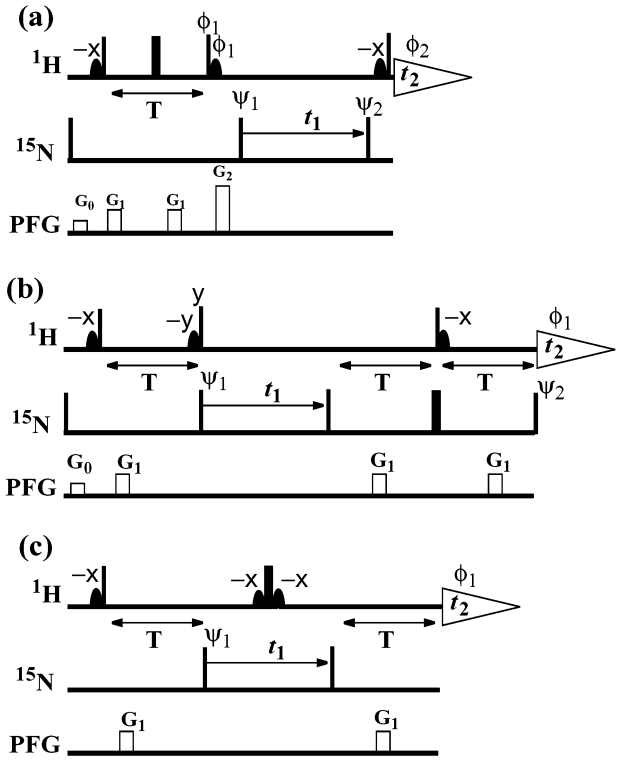

Figure 2. 2D [^{15}N,^{1}H]-correlation experiments using CRIPT or CRINEPT. (a) 2D [^{15}N,^{1}H]-CRIPT-TROSY. (b) 2D [^{15}N,^{1}H]-CRINEPT-TROSY. (c) 2D [^{15}N,^{1}H]-CRINEPT-HMQC-[^{1}H]-TROSY. In all three experiments the radio frequency pulses on ^{1}H and ^{15}N were applied at 4.8 and 119 ppm, respectively. The narrow and wide black bars indicate nonselective 90° and 180° pulses. The curved shapes on the ^{1}H line represent Gaussian-shaped selective 90° pulses on the water resonance, which have a length of 0.7−1.0 ms. The power and the phase of each water-selective pulse were adjusted by a trial-and-error approach to ensure an optimal alignment of the water magnetization along the *z*-axis during the entire experiment (see text). On the line marked PFG, rectangles indicate the duration and amplitude of pulsed magnetic field gradients applied along the *z*-axis: G_0, 500μs, 11 G/cm; G_1, 300 μs, 19 G/cm; G_2, 300 μs, 39 G/cm. Quadrature detection in the t_1(^{15}N) dimension is achieved by the States−TPPI method[31] applied to the phase ψ_1. The length of the period *T* was adjusted in the range 1.0−5.4 ms, depending on the size of the structure studied (see text). All radio frequency pulses are applied with phase x, unless a different phase is indicated in the figure: (a) ϕ_1 = {x, x, −x, −x}, ϕ_2 = {−x, x, x, −x, x, −x, −x, x}, ψ_1 = {x, −x}, ψ_2 = {x, x, x, x, −x, −x, −x, −x}. (b) ϕ_1 = {x, −x}, ψ_1 = {x, −x}; two free induction decays are recorded for each t_1 increment, with ψ_2 = {x, x} and ψ_2={−x, −x}, respectively, and are added with a 90° phase shift in both dimensions. (c) ϕ_1 = {x, −x}, ψ_1 = {x, −x}.

between ^{15}N−^{1}H^N dipole−dipole coupling and ^{1}H^N chemical shift anisotropy (CSA) during the time period *T*:[4,18]

$$\langle 2H_yN_z\rangle(T) = \sinh(R_{cor}T)\exp(-R_HT)\langle H_y\rangle(0) \quad (1)$$

with

$$R_H = \left[\frac{2}{9}(\gamma_H B_0 \Delta\sigma_H)^2 + \frac{1}{2}(\hbar\,\gamma_H\gamma_N/r_{HN}^3)^2\right]\frac{2}{5}\tau_c + \frac{1}{2T_1(N)} + \frac{1}{T_{2r}(H)} \quad (2)$$

and

$$R_{cor} = \frac{2}{3}(\gamma_H B_0 \Delta\sigma_H)(\hbar\,\gamma_H\gamma_N/r_{HN}^3)P_2(\vartheta)\frac{2}{5}\tau_c \quad (3)$$

H and N stand for ^{1}H^N and ^{15}N, R_H is the transverse relaxation rate of ^{1}H^N, and R_{cor} is the relaxation rate due to cross correlation between ^{1}H^N CSA (first term of eq 3) and ^{15}N−^{1}H dipole−dipole coupling (second term of eq 3). The Legendre polynome of the second order, $P_2(\vartheta)$, accounts for deviations of the angle ϑ between the dipole−dipole vector and the principal axis of the CSA tensor from 0°. The term $1/T_1$(N) is the longitudinal relaxation rate of ^{15}N, and $1/T_{2r}$(H) is the contribution to the transverse relaxation rate of ^{1}H^N due to dipole−dipole coupling with remote protons, H_i, at distances r_{HHi}. During the CRIPT transfer time, *T*, the proton chemical shift evolution is refocused by a 180° pulse, which also decouples the protons from ^{15}N. At the end of the period *T*, 90° pulses on ^{15}N and ^{1}H generate heteronuclear antiphase coherence $2H_z^NN_y$, which is then frequency-labeled during t_1. The hard 90° pulses on ^{15}N and ^{1}H applied at the end of t_1 transfer the coherences back to antiphase coherence $2H_Y^NN_z$, which is acquired during t_2. To minimize the overall length of the pulse sequence, no multiplet component selection is applied. In principle, the 2D [^{15}N,^{1}H]-CRIPT-TROSY experiment, thus, retains all four multiplet components of the ^{15}N−^{1}H-moieties, with two negative components upfield shifted and two positive components downfield shifted along the ^{1}H chemical shift axis (Table 1). In the practice of experiments with molecular sizes of about 200 kDa and above, however, transverse relaxation largely suppresses the unwanted three multiplet components.[3] The water magnetization is kept along the *z*-axis during the whole duration of the experiment, using the three water-selective pulses indicated by curved shapes in Figure 2a. The phase cycling scheme proposed in an earlier version of the 2D [^{15}N,^{1}H]-CRIPT-TROSY experiment (Figure 2a of ref 4) was extended to achieve improved suppression of artifacts.

The CRIPT delay, *T*, needs to be adjusted for the molecular size studied, since cross-correlated relaxation between dipole−dipole coupling and CSA increases with increasing rotational correlation time τ_c.[4] On the basis of eq 1, *T* is given by

$$T = \frac{1}{R_{cor}}\mathrm{ArcCosh}\left[\frac{R_H}{\sqrt{R_H^2 - R_{cor}^2}}\right] \quad (4)$$

Assuming for large structures that $1/T_{2r}(H) = \sum_i(\hbar\gamma_H^2/2r_{HH_i}^3)^2\tau_c \gg 1/T_1(N)$, one then has from eq 4 that *T* is, to a good approximation, inversely proportional to the effective rotational correlation time τ_c (see the additional data given in Figure 5). As these considerations imply, the

Table 1. Survey of the Salient Features of the Presently Described Solution NMR Experiments for Studies of Large Structures

Experiment	Polarization Transfer			Evolution/Acquisition		
	Nr[a]	Mechanism[b]	TROSY[c]	TROSY[c] t_1	TROSY[c] t_2	Peak Selection[d]
[^{15}N,^{1}H]-TROSY	3	$^3J_{HN}$	-	+	+	
[^{15}N,^{1}H]-CRIPT-TROSY	1	R_{cor}	+	+	+	
[^{15}N,^{1}H]-CRINEPT-TROSY	2[e]	$^3J_{HN}$+ R_{cor}	+	+	+	
[^{15}N,^{1}H]-CRINEPT-HMQC-[^{1}H]-TROSY	2	$^3J_{HN}$+ R_{cor}	+	-	+	

[a] Number of polarization transfers. [b] The term $^3J_{HN}$ indicates polarization transfer based on scalar couplings (INEPT);[24] R_{cor} indicates polarization transfer based on cross-correlated relaxation (CRIPT) (see text). [c] "+" indicates that transverse relaxation optimization is active; "−" sign indicates that there is no transverse relaxation optimization. [d] The square indicates the positions of the four multiplet components of a ^{15}N−^{1}H two-spin sytem in a non-decoupled [^{15}N−^{1}H]-correlation experiment. The ω_1(^{15}N) frequency is along the horizontal axis. The multicomponents selected by the individual experiments are indicated by "+" for positive intensity and "−" for negative intensity, and the sizes of the circles indicate the anticipated relative peak heights. [e] There are three periods *T* in the pulse sequence (Figure 2b), of which the second one is used for the multiplet component selection (see text).

(18) Brüschweiler, R.; Ernst, R. R. *J. Chem. Phys.* **1991**, *96*, 1758−1766.

2D [^{15}N,^{1}H]-CRIPT-TROSY experiment (Figure 2a) yields good results for very large structures, with molecular weights beyond 200 kDa.

Two-Dimensional [^{15}N,^{1}H]-CRINEPT-TROSY. The 2D [^{15}N,^{1}H]-CRINEPT-TROSY experiment (Figure 2b) provides an alternative as well as a complementation of 2D [^{15}N,^{1}H]-CRIPT-TROSY for studies of structures with molecular weights larger than 200 kDa. During CRINEPT-based polarization transfers, transverse relaxation−optimization is active and polarization is transferred via a combination of cross-correlated relaxation and scalar coupling.[4] Similar to the case of 2D [^{15}N,^{1}H]-CRIPT-TROSY, 2D [^{15}N,^{1}H]-CRINEPT-TROSY includes transverse relaxation−optimization during its entire duration (Table 1, Figure 2b). 2D [^{15}N,^{1}H]-CRINEPT-TROSY contains two CRINEPT transfer periods and a third delay of length T (Figure 2b) which is used to select for those two multiplet components of the ^{15}N−^{1}H four-line fine structure that have the slowest and fastest transverse relaxation rates (Table 1). Since no pulses are applied during the CRINEPT elements (Figure 2b), there is free proton chemical shift evolution, which leads to a sensitivity loss by a factor 2 when the coherence from the first CRINEPT element is refocused during the second CRINEPT element. A detailed description of the 2D [^{15}N,^{1}H]-CRINEPT-TROSY experiment is presented in ref 4.

Two-Dimensional [^{15}N,^{1}H]-CRINEPT-HMQC-[^{1}H]-TROSY. The 2D [^{15}N,^{1}H]-CRINEPT-HMQC-[^{1}H]-TROSY experiment[4] (Figure 2c) is included here as an alternative to 2D [^{15}N,^{1}H]-CRINEPT-TROSY that has higher intrinsic sensitivity (heteronuclear multiple-quantum correlation, HMQC). This is due to the fact that there is no loss of magnetization attributable to the proton chemical shift evolution during the two CRINEPT elements, since the chemical shift evolution is refocused with a 180° ^{1}H pulse. Part of this advantage is offset because there is no TROSY compensation during t_1, which results in broad resonances along the ^{15}N dimension. Since decoupling is applied during t_1 but not during acquisition (Figure 2c), there are two multiplet peaks per ^{15}N−^{1}H-moiety, which are shifted about 45 Hz (= 0.5 $^{1}J_{HN}$) upfield along the ^{15}N chemical shift axis when compared to the TROSY component (Table 1); that is, their position along ω_1(^{15}N) corresponds to that of the single peak in conventional, broad-band-decoupled COSY spectra.[3,15]

Results and Discussion

Conventional NMR spectra of large molecular structures in solution have broad natural line widths, and the ensuing poor resolution and sensitivity impose upper size limits for particular experiments. In the time domain, these deleterious features of the frequency spectrum correspond to rapid transverse relaxation. TROSY reduces the transverse relaxation rates during the frequency-labeling and acquisition periods, which results in improved resolution and sensitivity of the NMR experiments.[3] For structures in the molecular weight range up to about 150 kDa, this TROSY effect is sufficient for obtaining workable correlation spectra,[3,19] triple resonance spectra for sequential resonance assignments,[11,20,21] and NOESY spectra for resonance assignments and the collection of conformational constraints.[22] For larger structures, rapid transverse relaxation during the polarization transfer periods leads to a virtually complete loss of intensity for most signals. This is illustrated with the [^{15}N,^{1}H]-TROSY spectrum of the 800 kDa ^{15}N,^{2}H-labeled protein GroEL, where only about 20 resonances are observed (Figure 3a), which have been tentatively assigned to a C-terminal tail that is disordered in the X-ray crystal structure.[7] In contrast, relaxation optimization throughout the entire duration of the pulse sequence in 2D [^{15}N,^{1}H]-CRIPT-TROSY results in the acquisition of numerous [^{15}N,^{1}H]-correlation peaks from the structured part of ^{15}N,^{2}H-labeled GroEL (Figure 3b). Similar results to those of Figure 3b have been obtained with the 2D [^{15}N,^{1}H]-CRINEPT-TROSY and 2D [^{15}N,^{1}H]-CRINEPT-HMQC-[^{1}H]-

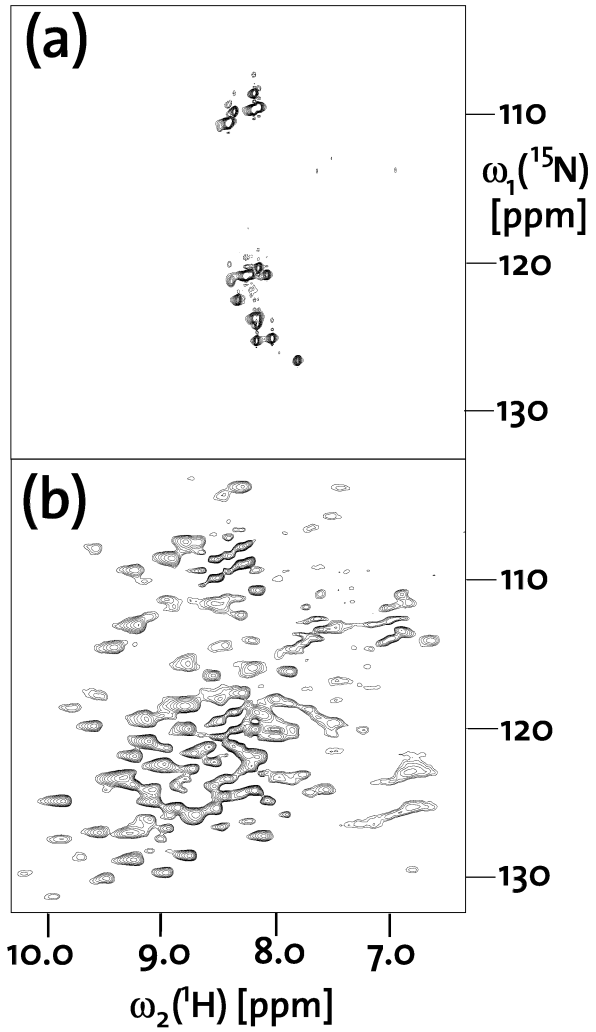

Figure 3. Heteronuclear 2D [^{15}N,^{1}H]-correlation spectra of the uniformly ^{15}N,^{2}H-labeled 800-kDa tetradecamer protein GroEL from *E. coli*. (a) 2D [^{15}N,^{1}H]-TROSY spectrum, measuring time = 20 h, acquired data size 256 × 1024 complex points, $t_{1,max}$ = 32 ms, $t_{2,max}$ = 100 ms. (b) 2D [^{15}N,^{1}H]-CRIPT-TROSY spectrum, measuring time = 20 h, acquired data size 100 × 1024 complex points, $t_{1,max}$ = 10 ms, $t_{2,max}$ = 100 ms. Prior to Fourier transformation, the data were multiplied along the t_1-dimension with a sine function shifted by 10° (ref 32) and in the t_2-dimension with an empirically optimized exponential function.

(19) Czisch, M.; Boelens, R. *J. Magn. Reson.* **1998**, *134*, 158−160. Pervushin, K.; Wider, G.; Wüthrich, K. *J. Biomol. NMR* **1998**, *12*, 345−348. Rance, M.; Loria, J. P.; Palmer, A. G. *J. Magn. Reson.* **1999**, *136*, 92−101. Zhu, G.; Kong, X. M.; Sze, K. H. *J. Biomol. NMR* **1999**, *13*, 77−81.
(20) Salzmann, M.; Pervushin, K.; Wider, G.; Senn, H.; Wüthrich, K. *Proc. Natl. Acad. Sci. U.S.A.* **1998**, *95*, 13585−13590.
(21) Loria, J. P.; Rance, M.; Palmer, A. G. *J. Magn. Reson.* **1999**, *141*, 180−184. Salzmann, M.; Wider, G.; Pervushin, K.; Wüthrich, K. *J. Biomol. NMR* **1999**, *15*, 181−184. Salzmann, M.; Wider, G.; Pervushin, K.; Senn, H.; Wüthrich, K. *J. Am. Chem. Soc.* **1999**, *121*, 844−848. Yang, D.; Kay, L. E. *J. Am. Chem. Soc.* **1999**, *121*, 2571−2575. Yang, D.; Kay, L. E. *J. Biomol. NMR* **1999**, *13*, 3−10. Mulder, A. A. F.; Ayed, A.; Yang, D.; Arrowsmith, C. H.; Kay, L. E. *J. Biomol. NMR* **2000**, *18*, 173−176. Permi, P.; Annila, A. *J. Biomol. NMR* **2001**, *20*, 127−133. Meissner, A.; Sorensen, O. W. *J. Magn. Reson.* **2001**, *150*, 100−104. Eletsky, A.; Kienhofer, A.; Pervushin, K. *J. Biomol. NMR* **2001**, *20*, 177−180.
(22) Meissner, A.; Sorensen, O. W. *J. Magn. Reson.* **1999**, *140*, 499−503. Pervushin, K.; Wider, G.; Riek, R.; Wüthrich, K. *Proc. Natl. Acad. Sci. U.S.A.* **1999**, *196*, 9607−9612. Zhu, G.; Xia, Y. L.; Sze, K. H.; Yan, X. Z. *J. Biomol. NMR* **1999**, *14*, 377−381. Xia, Y. L.; Sze, K. H.; Zhu, G. *J. Biomol. NMR* **2000**, *18*, 261−268.

TROSY experiments. In the following, we describe details of the setup of these experiments for measurements with very large structures. In particular, we will discuss the influence of the water handling on the sensitivity of the experiments (Figure 1), the optimization of the polarization transfer period, and the adjustment of the recycle delay. This will be followed by a comparative assessment of the performance of the different pulse schemes of Figure 2.

Water Suppression with Flip-Back Pulses. The dramatic influence of the selection of the water suppression scheme on the sensitivity of NMR experiments with large structures is illustrated with the 1D ^{1}H NMR experiment of Figure 1a, which contains a selective water flip-back pulse followed by a 90° (^{1}H) pulse and acquisition, so that the water magnetization is kept along the $+z$-axis during the whole experiment. The 1D ^{1}H NMR spectrum of uniformly ^{15}N,^{2}H-labeled GroEL recorded with this pulse sequence contains a broad envelope with sizable intensity from about 6 to 10 ppm (Figure 1b). The corresponding ^{1}H NMR spectrum recorded with solvent suppression by presaturation during the recycle delay shows similar features, except that the signal intensity is reduced about 10-fold. Similar sensitivity losses were observed in multidimensional experiments with less than optimal water suppression (data not shown). All our NMR experiments for large structures, therefore, used water flip-back techniques with an individual adjustment of each individual water-selective pulse, as described in Methods.

The dramatic influence of the water handling on the intensities of the protein signals implicates strong interactions between the water magnetization and the protein magnetization, which affect the effective longitudinal ^{1}H relaxation rate[23] (M. Hohwy, D. Braun, G. Wider and K. Wüthrich, to be published).

Adjusting the Polarization Transfer Periods. The spectra of ^{15}N,^{2}H-labeled GroEL in Figure 3 show that transverse relaxation optimization process during the polarization transfers is indispensable in NMR experiments with large structures. In all the experimental schemes of Figure 2, the standard insensitive nuclei enhanced by polarization transfer (INEPT)[24] has, therefore, either been supplemented or substituted by a transfer scheme based on cross-correlated relaxation.[4,18] Although the rate of J-coupling-based INEPT transfers is independent of molecular size, the transverse relaxation rate during the transfer increases for larger structures in such a way as to reduce the overall efficiency of the INEPT transfer. In contrast, the rate of cross-correlated relaxation-induced polarization transfers increases for larger values of the correlation time, τ_c, and the optimal transfer time decreases, so that CRIPT transfers become more efficient for large molecules, although the maximum extent of transfer of 0.5 is independent of τ_c (eqs 2−4).[4] Figure 4a and b illustrates the experimental determination of the optimal CRIPT time for SR1 and GroEL. The black squares in Figure 5 represent the, thus, measured optimal transfer times for five structures with estimated τ_c-values between 50 and 350 ns. The experimental data have been approximated with a model calculation described in the figure caption 5, and the resulting smooth curve in Figure 5 provides a starting point for estimating the delay to be used in the experiments of Figure 2 for a given system. In our experience, however, it is worthwhile to measure new CRIPT build-up curves (Figure 4a and b) for optimizing the transfer delays in each new system studied.

Measurement of the optimal CRIPT transfer period T can also be used, via the curve in Figure 5, to estimate the overall

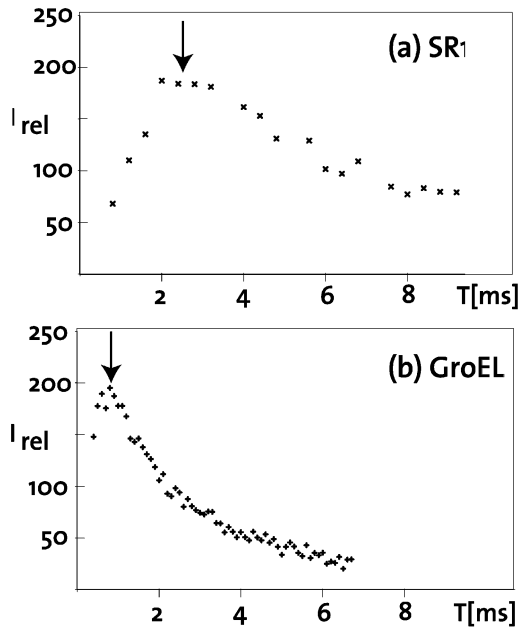

Figure 4. Experimental measurement of the CRIPT transfer efficiency at a proton frequency of 750 MHz. (a) Plot of the relative NMR peak heights, I_{rel}, as a function of the duration of the CRIPT transfer for the 400-kDa protein SR1. The buildup curve was obtained from a series of measurements with the pulse sequence of Figure 2a. The transfer delay, T, was incremented stepwise from 0.8 to 9.0 ms between the individual experiments. (b) Same as part a for the 800-kDa protein GroEL. T was incremented between 0.4 and 6.8 ms. The arrows indicate the T values with optimal transfer efficiency that were derived from these data (see also Figure 5).

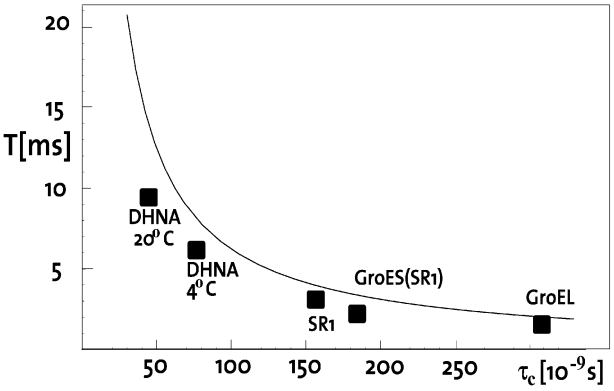

Figure 5. CRIPT transfer delays, T (Figure 2a), providing optimal transfer efficiency at a proton frequency of 750 MHz. The black squares represent experimental optimal T-values measured with the experiments of Figure 4 for the following ^{15}N,^{2}H-labeled proteins: DHNA (110 kDa, estimated value for τ_c = 45 ns at 20 °C and 75 ns at 4 °C), SR1 (400 kDa, τ_c = 155 ns at 25 °C), GroES in a complex with SR1 (472 kDa, τ_c = 185 ns at 25 °C), GroEL (800 kDa, τ_c = 310 ns at 35 °C). The τ_c values were estimated from the molecular weight and the temperature used, assuming a rigid spherical shape of the structures studied, and the previously reported experimental τ_c values for DHNA[4] were used as an additional reference. The experimental data were fitted using eq 4 (see also eqs 1−3) with the following parameters: r_{HN} = 1.04 Å, $\Delta\sigma_H$ = 15 ppm, ϑ = 10°, dipole−dipole coupling with the remote protons expected in an α-helix, that is, $^1H^N(i\text{-}2)$, $^1H^N(i\text{-}1)$, $^1H^N(i+1)$, and $^1H^N(i+2)$ at distances of 4.2, 2.8, 2.8, and 4.2 Å, respectively.[2,20]

(23) Wang, Y. X.; Jacob, J.; Cordier, F.; Wingfield, P.; Stahl, S. J.; Lee-Huang, S.; Torchia, D.; Grzesiek, S.; Bax, A. *J. Biomol. NMR* **1999**, *14*, 181−184. Koenig, S. H.; Bryant, R. G.; Hallenga, K.; Jacob, G. S. *Biochemistry* **1978**, *17*, 4348−4358. Ceckler, T. L.; Balaban, R. S. *J. Magn. Reson. B* **1994**, *105*, 242−248.
(24) Morris, G. A.; Freeman, R. *J. Am. Chem. Soc.* **1979**, *101*, 760−762.

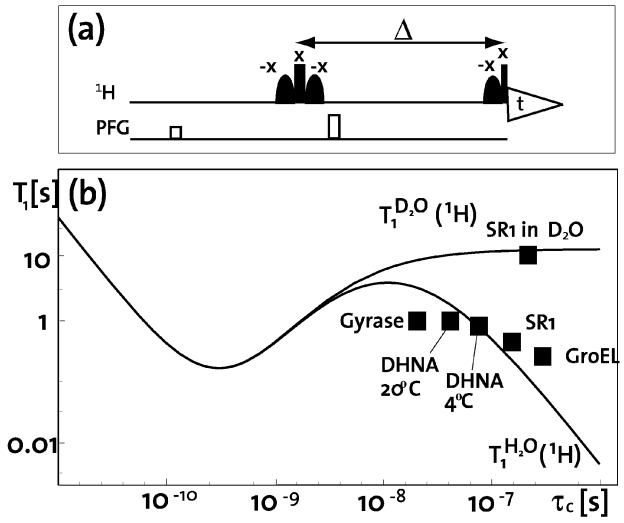

Figure 6. Measurement of the longitudinal proton relaxation times $T_1(^1H)$ for a selection of proteins in the size range 40−800 kDa. (a) Pulse sequence used to measure $T_1(^1H)$. The experiment starts with a 180° pulse, which is followed by the recovery delay Δ and a 90° observation pulse. The water resonance is held along $+z$ during the entire experiment by applying three water-selective 90° pulses, which are indicated by the curved shapes before and after the 180° pulse and before the 90° hard pulse. The pulsed magnetic field gradients during the interscan delay and the recovery delay had a duration of 1 ms and amplitudes of 10 and 20 G/cm, respectively. (b) The black squares represent experimental $T_1(^1H)$ values measured at 400 MHz on a Varian INOVA spectrometer for the following ^{15}N,^2H-labeled proteins: Gyrase (43 kDa, estimated $\tau_c = 17$ ns at 20 °C), DHNA (at 4° and 20 °C), SR1 (at 20 °C), and GroEL (at 20 °C) (for details on these proteins, see caption to Figure 5). For each structure, 30 measurements were recorded with the pulse sequence of part a, using recovery delays Δ between 10 ms and 3 s. The experimental relaxation time $T_1^{D_2O}(^1H)$ at a proton frequency of 400 MHz was fitted using eqs 5−8 with the following model assumptions: We consider a $^{15}N-^1H$ group located in a β-sheet, with the remote protons $^1H^N(i-1)$, $^1H^N(i+1)$, and $^1H^N(j)$ at distances of 4.3, 4.3, and 3.3 Å, respectively,[2] fast internal motion with $\tau_e = 100$ ps, and order parameter $S^2 = 0.8$.[29] For the fit of the $T_1^{H_2O}$ data, an additional remote proton was introduced, which is assumed to be in fast exchange with the bulk water at a distance of 4.0 Å, so that it is in Boltzmann equilibrium.

rotational correlation time τ_c of a new structure. Although this procedure enables only an approximate estimate of the τ_c value because of the variation of the ^1H chemical shift anisotropy tensors along the polypeptide chain,[25] it is of practical interest as a substitute for the standard method of calculating τ_c from the ratio of $T_1(^{15}N)$ and $T_2(^{15}N)$[15]. The latter approach is usually impractical for large structures, because of the low sensitivity of the experiments used to measure the relaxation times.

Adjustment of the Recycle Delay. The adjustment of the relaxation delay, Δ, for obtaining maximal sensitivity of an NMR experiment within a given total measuring time is primarily based on considerations of the effective longitudinal relaxation times and the desirable pulse rotation angle.[26] To obtain a basis for estimating a favorable recycle time for the setup of the experiments in Figure 2, we measured the proton T_1-values of a group of structures with molecular weights from 40 to 800 kDa (Figure 6) in H_2O solution. For GroEL, the value of the effective longitudinal relaxation time in H_2O, $T_1^{H_2O}(^1H)$, was thus found to be 0.3 s; for SR1, it was 0.4 s, and for DHNA at 20 °C, it was 0.8 s. Overall, for τ_c values longer than about 100 ns, a plot of the experimental $T_1^{H_2O}(^1H)$ values versus the overall rotational correlation time τ_c levels off and even shows a trend toward shorter $T_1^{H_2O}(^1H)$ values for larger sizes. The experimental values for $T_1^{H_2O}(^1H)$ in Figure 6 are also much shorter than what one would predict from the formalism of established relaxation theory.[26,27] This apparent discrepancy appears to be the result of intramolecular motions and exchange-mediated interactions with the solvent water that are not properly accounted for in conventional relaxation theory[23] (M. Hohwy, D. Braun, G. Wider and K. Wüthrich, to be published). The presence of a strong coupling between the water ^1H magnetization and the ^1H magnetization of the macromolecular solute is supported by the observation that the effective longitudinal relaxation time for SR1 in D_2O solution, $T_1^{D_2O}(^1H) = 6$ s, is much longer than the value measured in H_2O solution (Figure 6b). Furthermore, the longitudinal relaxation times of amide protons measured in H_2O solution increased up to 5-fold when the water resonance was saturated during the recovery delay Δ (Figure 6a) (data not shown; see Figure 1).

An approximate qualitative fit of the experimental data in H_2O and D_2O solutions (Figure 6b) was obtained with the following model calculations, which account for the overall rotational tumbling of a solid sphere representing the structure considered and for the intramolecular mobility of the $^{15}N-^1H$ groups within the structure. The longitudinal proton relaxation time for amide protons in a protein in D_2O solution, $T_1^{D_2O}(^1H)$, was calculated from eqs 5−7:[28]

$$1/T_1^{D_2O}(^1H) = (\hbar\,\gamma_H\gamma_N/2r_{HN}^3)^2[J(\omega_H - \omega_N) + 3J(\omega_H) + 6J(\omega_H + \omega_N)] + \frac{1}{3}(\gamma_H B_0 \Delta\sigma_H)^2 J(\omega_H) + \rho_{HH} + \sigma_{HH} \quad (5)$$

$$\rho_{HH} = \sum_i (\hbar\,\gamma_H^2/2r_{HH_i}^3)^2[J(0) + 3J(\omega_H) + 6J(2\omega_H)] \quad (6)$$

$$\sigma_{HH} = \sum_i (\hbar\gamma_H^2/2r_{HH_i}^3)^2[-J(0) + 6J(\omega_H)] \quad (7)$$

Equations 6 and 7 account for auto- and cross-relaxation due to dipole−dipole coupling to i remote hydrogen nuclei at distances r_{HH_i}. r_{HN} is the distance between the covalently linked ^1H and ^{15}N spins, $\Delta\sigma_H$ is the CSA tensor of nucleus ^1H, B_0 is the static magnetic field, $\hbar$ is the Planck constant divided by 2π, γ_H and γ_N are the gyromagnetic ratios of ^1H and ^{15}N, and ω_H and ω_N are the Larmor frequencies of ^1H and ^{15}N, respectively. The spectral density is given by[15]

$$J(\omega) = \frac{2}{5}\frac{S^2\tau_c}{1 + (\tau_c\omega)^2} + \frac{2}{5}\frac{(1-S)^2\left(\frac{\tau_c\tau_e}{\tau_c + \tau_e}\right)}{1 + \left(\frac{\tau_c\tau_e}{\tau_c + \tau_e}\omega\right)^2} \quad (8)$$

with the internal correlation time τ_e and the order parameter S^2.[29] The measured mean value of $T_1^{D_2O}$ in SR1 was satisfactorily approximated with the use of an order parameter $S^2 =$

(25) Tjandra, N.; Bax, A. *J. Am. Chem. Soc.* **1997**, *119*, 8076−8082. Tessari, M.; Mulder, F. A. A.; Boelens, R.; Vuister, G. W. *J. Magn. Reson.* **1997**, *127*, 128−133. Tessari, M.; Mulder, F. A. A.; Boelens, R.; Vuister, G. W. *J. Am. Chem. Soc.* **1997**, *119*, 8985−8990.
(26) Ernst, R. R.; Bodenhausen, G.; Wokaun, A. *The Principles of Nuclear Magnetic Resonance in One and Two Dimensions;* Clarendon: Oxford, U.K., 1987.
(27) Abragam, A. *The Principles of Nuclear Magnetism;* Clarendon: Oxford, U.K., 1961.
(28) Wagner, G. *Curr. Opin. Struct. Biol.* **1993**, *3*, 748−754.

0.8 and an internal correlation time $\tau_e = 100$ ps in eqs 5−8 (Figure 6b). For a satisfactory fit of the relaxation times measured in a H_2O solution, the overall relaxation rate was expressed by eq 9,

$$1/T_1^{H_2O}(^1H) = 1/T_1^{D_2O}(^1H) + \rho_{HH^O} \quad (9)$$

ρ_{HH^O} accounts for dipole−dipole coupling to the additional remote hydrogen nuclei $^1H°$, which are assumed to be in fast exchange with the bulk water so that they would not be seen in D_2O solution. Examples would be the hydroxyl protons of Thr, Tyr, and Ser.[2] In eq 9, it is assumed that the exchange of $^1H°$ with the bulk water is sufficiently fast, so that cross relaxation between $^1H^N$ and $^1H^O$ is negligibly small. The smooth curve in Figure 6 was obtained with the assumption that a single $^1H^O$ spin in fast exchange with the bulk water is present at a distance of 4.0 Å from the observed $^1H^N$ spin.

$T_1^{D_2O}$ and $T_1^{H_2O}$ are similar for τ_c values shorter than about 5 ns, whereas the interaction with remote protons in fast exchange with H_2O becomes dominant for long τ_c values. In practice, the smooth curves in Figure 6 provide a starting point for estimating the relaxation delay Δ for new structures with known molecular weight.

Comparison of the 2D [^{15}N,^{1}H]-CRINEPT-TROSY, 2D [^{15}N,^{1}H]-CRINEPT-HMQC-[^{1}H]-TROSY, and 2D [^{15}N,^{1}H]-CRIPT-TROSY Experiments. In the 2D [^{15}N,^{1}H]-TROSY spectrum of the ^{15}N,^{2}H-labeled heptameric 72-kDa protein GroES, 89 out of the 94 expected ^{15}N−^{1}H signals have been observed.[30] For ^{15}N,^{2}H-labeled GroES in a complex with ^{2}H-labeled SR1, which has a molecular weight of 472 kDa, 78 of the expected 94 cross-peaks are detected in the 2D [^{15}N,^{1}H]-CRINEPT-TROSY, 2D [^{15}N,^{1}H]-CRINEPT-HMQC-[^{1}H]-TROSY and 2D [^{15}N,^{1}H]-CRIPT-TROSY spectra (Figure 7), showing that TROSY-optimization throughout the entire pulse sequence (Table 1) enables the recording of virtually complete ^{15}N−^{1}H fingerprints for a structure size of nearly 500 kDa. The following is a more detailed evaluation of the relative merits of the three experiments of Figure 2 for studies of very large structures.

The 2D [^{15}N,^{1}H]-CRINEPT-HMQC-[^{1}H]-TROSY experiment uses CRINEPT to detect cross-peaks of ^{15}N−^{1}H-moieties from both flexible and more rigidly structured protein regions. The peaks have broad line widths along the $\omega_1(^{15}N)$ dimension because of the absence of TROSY-compensation in the indirect dimension (Table 1), and there is probably also a contribution to the line widths from dipolar coupling of the multiple quantum states to remote protons. This is clearly seen when the 2D [^{15}N,^{1}H]-CRINEPT-HMQC-[^{1}H]-TROSY spectrum is processed identically to the data sets of Figure 7b and c (Figure 8). With the digital filtering of Figure 7a, a similar spectrum could be generated as for the fully TROSY-based spectra of Figure 7b and c, but this processing also introduced artifactual "wiggles" of the most intense cross-peaks (Figure 9), which correspond to mobile ^{15}N−^{1}H-groups in a loop of the protein. For flexible ^{15}N−^{1}H-moieties, one also observes two multiplet components (Table 1), whereas, for cross-peaks from structured regions of the protein, the rapid transverse relaxation suppresses the lower-field fine structure component (Figure 7a). Overall, the 2D [^{15}N,^{1}H]-CRINEPT-HMQC-[^{1}H]-TROSY experiment has been used primarily for the initial screening of the feasibility of NMR

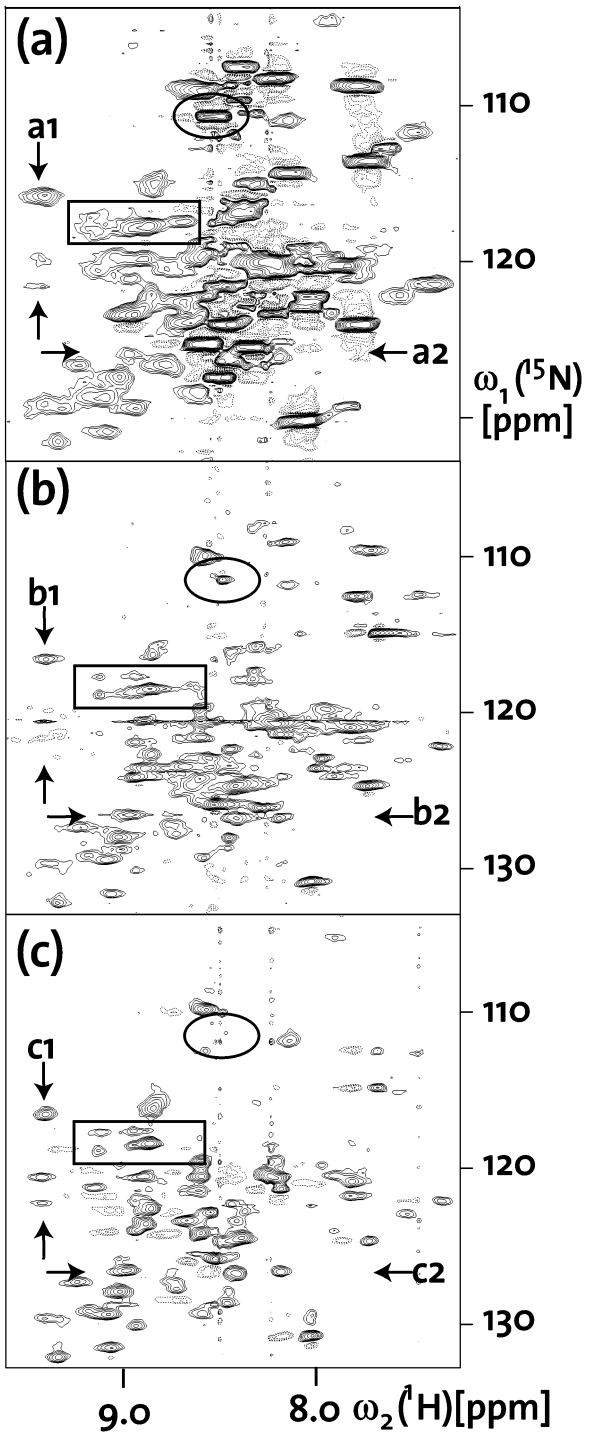

Figure 7. 2D [^{15}N,^{1}H]-correlation spectra recorded using the experimental schemes of Figure 2 with uniformly ^{15}N,^{2}H-labeled GroES bound to SR1 in a complex with molecular weight 472 kDa. (a) 2D [^{15}N,^{1}H]-CRINEPT-HMQC-[^{1}H]-TROSY. (b) 2D [^{15}N,^{1}H]-CRINEPT-TROSY. (c) 2D [^{15}N,^{1}H]-CRIPT-TROSY. A cross-peak corresponding to a mobile ^{15}N−^{1}H-group is circled. The rectangle indicates a spectral region that is discussed in the text. The arrows indicate the positions of the cross-sections shown in Figure 9. The acquired data size is 100 × 1024 complex points, with $t_{1,max} = 10$ ms and $t_{2,max} = 100$ ms. Prior to Fourier transformation, a sine bell was applied in the t_1-dimension, with phase shifts of 10° for part a and 30° for parts b and c,[32] and an empirically optimized exponential function was applied in the t_2-dimension.

(29) Lipari, G.; Szabo, A. *J. Am. Chem. Soc.* **1982**, *104*, 4546−4558.
(30) Fiaux, J.; Bertelsen, E. B.; Horwich, A. L.; Wüthrich, K. *Nature* **2002**, *418*, 207−211.
(31) Marion, D.; Ikura, K.; Tschudin, R.; Bax, A. *J. Magn. Reson.* **1989**, *85*, 393−399.
(32) DeMarco, A.; Wüthrich, K. *J. Magn. Reson.* **1976**, *24*, 201−204.

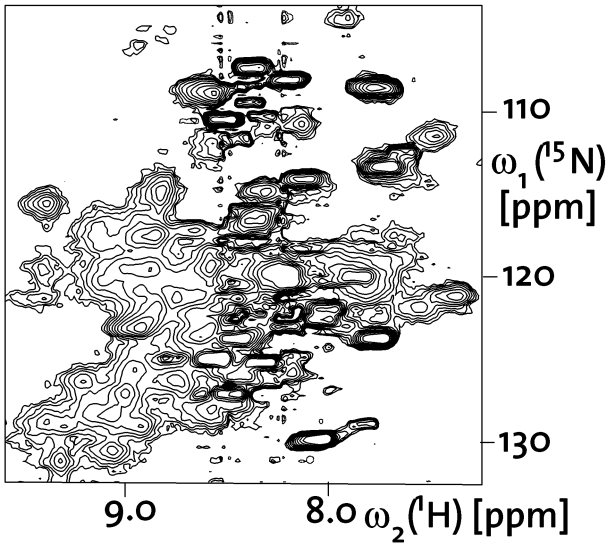

Figure 8. Illustration of the impact of different digital filterings on NMR spectra of large structures obtained with the experiments of Figure 2. Here, the data of the 2D [^{15}N,^{1}H]-CRINEPT-HMQC-[^{1}H]-TROSY experiment in Figure 7 have been treated identically to those of the 2D [^{15}N,^{1}H]-CRINEPT-TROSY and 2D [^{15}N,^{1}H]-CRIPT-TROSY experiments of Figure 7; that is, a sine bell shifted by 30° was applied along the t_1-dimension[32] (see text).

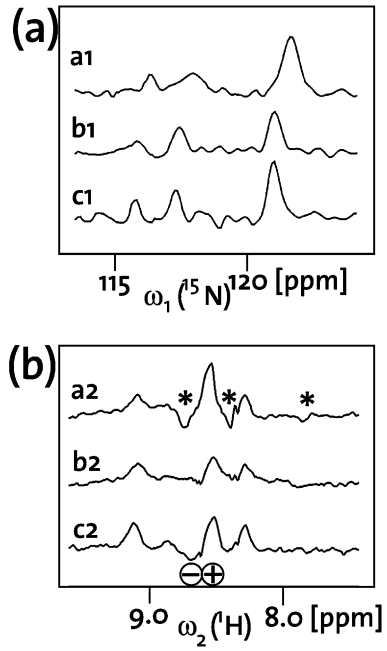

Figure 9. Cross-sections through the 2D ^{15}N−^{1}H correlation spectra of uniformly ^{15}N,^{2}H-labeled GroES bound to SR1. In Figure 7, the positions of the cross-sections are indicated by arrows and the appropriate lettering. The asterisks identify transformation artifacts due to the 10°-shifted sine bell function[32] used to enhance the resolution of the 2D [^{15}N,^{1}H]-CRINEPT-HMQC-[^{1}H]-TROSY spectrum (see Figures 7 and 8). The + and − signs below the trace c2 indicate the antiphase character of multiplets observed in the 2D [^{15}N,^{1}H]-CRIPT-TROSY spectrum.

observations with new structures, where one can exploit the intrinsic high sensitivity of this scheme.

The 2D [^{15}N,^{1}H]-CRINEPT-TROSY experiment uses CRINEPT transfers to ensure that cross-peaks of ^{15}N−^{1}H-moieties from flexible as well as structured regions of the protein are detected. Use of TROSY in both dimensions (Table 1) results in narrow line shapes. This is readily seen by comparison of the resolution in the spectral region highlighted by the rectangles in Figure 7. The 2D [^{15}N,^{1}H]-CRINEPT-TROSY experiment is somewhat less sensitive when compared to the other two experiments of Figure 2, because of the longer pulse sequence used for multiplet component selection (Table 1). For structure sizes above about 200 kDa, transverse relaxation ensures that only the TROSY-component of the remaining two-component multiplet (Table 1) is seen.

The 2D [^{15}N,^{1}H]-CRIPT-TROSY experiment with its single polarization transfer (Table 1) provides high sensitivity for the observation of peaks with fast transverse relaxation. These strong peaks then typically arise from ^{15}N−^{1}H-moieties located in well-structured regions of the protein core, whereas peaks originating from flexible loops or chain ends are suppressed. Similarly, peaks that might arise from admixtures of smaller protein impurities would be filtered away. The filtering effect can be fine-tuned with the experimental setup. For example, with a transfer delay of $T = 2.2$ ms, CRIPT selects for ^{15}N−^{1}H-moieties with an effective rotational correlation time τ_c longer than about 200 ns, which corresponds to a molecular weight of about 500 kDa. This is illustrated in Figure 7 with the circled cross-peak, which is only observable in the CRINEPT-based spectra of Figure 7a and b, but is suppressed in the 2D [^{15}N,^{1}H]-CRIPT-TROSY experiment of Figure 7c. Comparison with 2D [^{15}N,^{1}H]-TROSY spectra, where the peaks from amide protons with short transverse relaxation times are suppressed (Figure 3), confirmed that the missing peaks in Figure 7c originate from ^{15}N−^{1}H groups with slow transverse relaxation. A limitation of the 2D [^{15}N,^{1}H]-CRIPT-TROSY scheme arises because ^{15}N−^{1}H moieties with small ^{1}H CSA or a large angle ϑ may not be detected because of the absence or near-absence of cross-correlated relaxation, R_{cor} (eq 3). These peaks will normally be present in CRINEPT-based experiments and can, therefore, not a priori be distinguished from peaks representing either flexible regions of a large structure or admixtures of smaller proteins. At 472 kDa, an antiphase multiplet pattern (Table 1) is visible only for a small number of peaks (Figure 9), which all appear to originate from flexible loops. This demonstrates nicely that the multiplet component selection by rapid transverse relaxation works well for structures in the size range of interest for the use of the 2D [^{15}N,^{1}H]-CRIPT-TROSY experiment.

2D Correlation Spectra of ^{15}N,^{2}H-labeled GroEL. In the 800 kDa ^{15}N,^{2}H-labeled GroEL, the C-terminal 24-residue polypeptide segment is disordered[7] and probably highly flexible. This expectation from EM and X-ray studies is supported by the observation of a small number of strong resonances with random coil ^{1}H chemical shifts[2] in the 2D [^{15}N,^{1}H]-TROSY spectrum of GroEL and by the absence of these peaks in the 2D [^{15}N,^{1}H]-CRIPT-TROSY spectrum recorded with a CRIPT delay of $T = 1.4$ ms (Figure 3). On the other hand, the 2D [^{15}N,^{1}H]-CRIPT-TROSY spectrum contains a large number of cross-peaks which belong to ^{15}N−^{1}H-moieties with long rotational correlation times, τ_c (Figure 3), illustrating again that the 2D [^{15}N,^{1}H]-CRIPT-TROSY experiment is a powerful selection scheme for ^{15}N−^{1}H spin systems with long τ_c values.

The peaks in the 2D [^{15}N,^{1}H]-CRIPT-TROSY spectrum of ^{15}N,^{2}H-labeled GroEL recorded in H_2O (Figure 3b) account for only about 20% of the expected ^{15}N−^{1}H correlation peaks. This observation will be further investigated. At the present state of the investigation, we cannot exclude any of the following

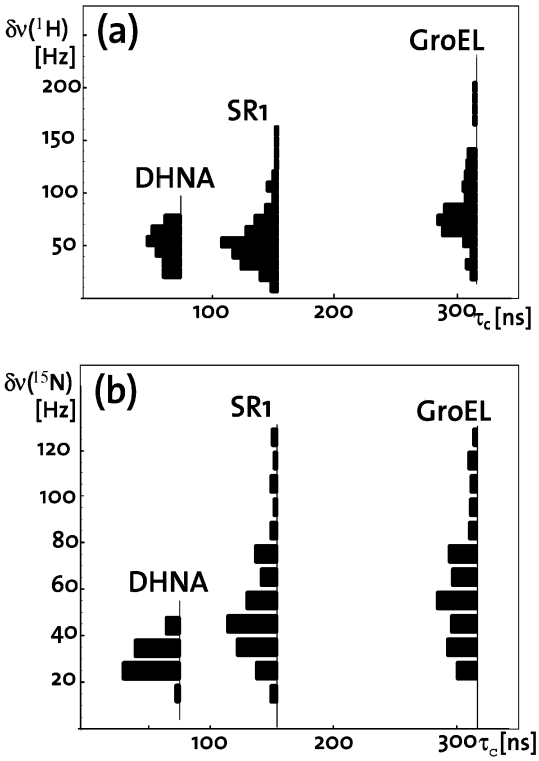

Figure 10. NMR line widths observed in 2D [^{15}N,^{1}H]-CRIPT-TROSY spectra of H_2O solutions of the proteins DHNA, SR1, and GroEL at a ^{1}H resonance frequency of 750 MHz. In parts a and b, respectively, the distributions of the ^{1}H and ^{15}N line widths are displayed by black bars which represent the number of peaks with a given line width along the vertical axis. As part of the data processing, a cosine window function was applied to the data in both dimensions prior to Fourier transformation. For SR1 and GroEL, only about 20% of the ^{15}N−^{1}H cross-peaks expected from the molecular structure were observed (see text).

possible explanations for the apparent paucity of observable signals. Since GroEL was expressed on a D_2O nutrient and has not been unfolded during the purification, some of the missing amide groups are probably not NMR-observable because they remain deuterated because of slow $^{2}H^{N}/^{1}H^{N}$ exchange. This explanation is supported by the observations that a few new peaks appeared after prolonged standing of the GroEL in H_2O solution and that perdeuterated GroES with complete protonation of the amide groups, as monitored by the NMR spectra of free GroES, in a complex with unlabeled GroEL yielded spectra containing nearly all expected cross-peaks.[30] Alternatively, the broad distribution of the line widths in GroEL (see the following section and Figure 10) suggests that some missing peaks might be broadened beyond detection.

^{15}N and ^{1}H Line Widths in TROSY-Type Experiments. The ^{15}N and ^{1}H line widths were measured in 2D [^{15}N,^{1}H]-CRIPT-TROSY spectra of H_2O-solutions of ^{15}N,^{2}H-labeled DHNA at 4 °C, ^{15}N,^{2}H-labeled SR1 at 25 °C, and ^{15}N,^{2}H-labeled GroEL at 25 °C (Figure 10). For DHNA, the average line widths are 50 Hz along the ^{15}N dimension and 30 Hz along the ^{1}H dimension. For SR1, average values of 60 Hz were observed for both the ^{15}N and ^{1}H line widths, and for GroEL, these quantities are 75 and 110 Hz, respectively. In the two larger proteins, SR1 and GroEL, we observed only approximately 20% of the total number of resonances expected from the chemical structure in the fully symmetric assemblies.[7−10] The observable resonances show a much broader line width distribution than DHNA, although the spectrum of DHNA contains nearly all of the expected peaks. We currently do not know whether the missing resonances in SR1 or GroEL escaped observation because of even broader line widths than the upper limit in Figure 10 or other factors, in particular line broadening by exchange processes, so that the line width distribution of Figure 10 could be biased. Nevertheless, these data should be useful as an indication of the line widths to expect when working with uniformly deuterated polypeptide chains in very large structures. The facts that the same subset of peaks observed for the 800 kDa GroEL is also seen for the 400 kDa SR1 (data not shown) and that the line width distribution is very broad in both cases (Figure 10) suggest that specific structural or dynamic features of the assembly of GroEL subunits into seven-membered rings might limit the NMR observation to a subset of the expected resonances. A somewhat different situation might be encountered with uniformly deuterated chains in different large supramolecular structures, as appears to be indicated by the observations with DHNA.

Conclusions

This paper shows how the combined use of TROSY during the frequency labeling and acquisition periods and CRINEPT or CRIPT for polarization transfer can be used as a basis for NMR studies of structures with molecular weights of 500 kDa and beyond. Among the four 2D correlation experiments considered, 2D [^{15}N,^{1}H]-TROSY enables the observation of resonance lines from amide groups in flexible chain ends or surface loops, whereas 2D [^{15}N,^{1}H]-CRIPT-TROSY suppresses these resonances and emphasizes the signals originating from well-structured parts of the proteins, which are subject to rotational diffusion on a time scale that is largely determined by the overall size of the structure. These two experiments, thus, provide a survey of all the resonance lines that may originate from a given structure. The two additional experiments, 2D [^{15}N,^{1}H]-CRINEPT-TROSY and 2D [^{15}N,^{1}H]-CRINEPT-HMQC-[^{1}H]-TROSY, which both use CRINEPT, provide a complete spectrum in a single experiment. The combination of the entire group of experiments is, thus, helpful for the spectral analysis, and the filtering effects of the 2D [^{15}N,^{1}H]-TROSY and 2D [^{15}N,^{1}H]-CRIPT-TROSY experiments provide direct information on dynamic properties of the molecular regions observed by these experiments.[4,30]

In Figures 5 and 6 and in the discussion on water suppression, we provide general guidelines for the setup of the experiments of Figure 2 for studies of structures in the molecular weight range from 200 to 800 kDa. We use these guidelines in our own work, but on the basis of the experience gained with GroES, SR1, and GroEL, we would like to re-emphasize that it is worthwhile to optimize the setup of these experiments anew for each new system studied, which may include a new calibration of the water flip-back pulses, new determination of the optimal polarization transfer time (Figure 4), and measurements of the longitudinal proton relaxation times.

Satisfactory results with the experiments in Figure 2 have so far been obtained with proteins that had been deuterated to the extent of at least 85%. As was mentioned in the text, limitations tend to arise from the fact that a large percentage of the amide groups in large structures may not readily be observable in ^{15}N,^{1}H-correlation experiments because of the incomplete

exchange of the deuterons from the nutrient medium in D_2O solution against protons, even after a long standing in H_2O solution. The implication is that among the large structures studied in this paper, GroEL, SR1, and GroES bound to SR1, only the SR1-bound GroES had completely protonated amide groups, as evidenced by the NMR spectra recorded with free GroES in H_2O solution.[30] The experiments with the GroES complexes with SR1 (Figures 7−9 and ref 30) and GroEL[30] are, therefore, of particular importance for the validation of the presently described experimental procedures.

Potential practical applications of the procedures described in this paper include investigations of the variable mobility in different parts of large macromolecular structures, the chemical shift mapping of intermolecular contact areas in supramolecular structures, and the use of the 2D [^{15}N,^{1}H]- fingerprints as a basis for the screening of potential drug molecules for binding to receptor structures in the size range of interest here. Variations of the chemical shifts in the [^{15}N,^{1}H]-fingerprints may further provide indications on conformational changes of a given macromolecular structure upon interactions with other molecules. In many of these potential applications, the apparent limitation arising from the lack of $^{2}H \rightarrow {}^{1}H$ exchange from the core of large proteins might even be used in support of particular projects, by providing a simplification of the spectra as well as initial indications for the assignment of the observed resonance lines to surface areas of the structure considered.

Acknowledgment. This work was supported by the Schweizerischer Nationalfonds (project 31.49047.96), by HHMI, and by NIH. We thank K. Furtak for help in constructing the plasmids used for the expressions of GroEL and SR1.

JA026763Z